

2<sup>nd</sup> CIRP 2nd CIRP Conference on Surface Integrity (CSI)Force-Based Temperature Modeling for Surface Integrity  
Prediction in Broaching Nickel-Based AlloysF. Klocke<sup>a</sup>, S. Gierlings<sup>a\*</sup>, M. Brockmann<sup>a</sup>, D. Veselovac<sup>a</sup><sup>a</sup> WZL Aachen, RWTH Aachen University, Steinbachstrasse 19, 52074 Aachen, Germany\* Corresponding author. Tel.: +49 241 80 20522; fax: +49 241 80 22293. E-mail address: [s.gierlings@wzl.rwth-aachen.de](mailto:s.gierlings@wzl.rwth-aachen.de).**Abstract**

Surface Integrity standards for safety-critical aero engine components are very high. Besides the properties of the work piece material, the selected process parameters for machining have a significant impact on the achieved part quality. The present article identifies thermal induced Surface Integrity parameters such as micro-hardness, white-etching-layers and increased residual tensile stress as most critical when broaching Nickel-based alloys and presents a force-based concept for temperature prediction. The achieved results with the new model approach are compared to in-process temperature measurements.

© 2014 The Authors. Published by Elsevier B.V. Open access under [CC BY-NC-ND license](#).Selection and peer-review under responsibility of The International Scientific Committee of the “2nd Conference on Surface Integrity” in the person of the Conference Chair Prof Dragos Axinte [dragos.axinte@nottingham.ac.uk](mailto:dragos.axinte@nottingham.ac.uk)**Keywords:** Machining; Surface Integrity; Temperature; Modeling**1. Introduction**

Across all sectors of industry as well as in science it is accepted that the quality of a machined feature is inevitably dependent on the cutting process, i.e. cutting conditions. For quality parameters such as geometric dimensions or kinematic surface roughness this relationship is perfectly obvious. In case of Surface Integrity parameters describing alterations in the work piece microstructure, correlations between cutting conditions and quality aspects are often unapparent and thus matter of current research projects.

The fact that machining processes in general are accompanied by tool wear is as much uncontroversial as observations that cutting conditions have a direct impact on tool life time as well as the wear phenomena. It is a question of perspective, whether tool wear is regarded as an output variable of certain process conditions over time or if tool wear is considered an aspect of cutting conditions itself – it is true, however, that tool wear has a major influence on part quality.

Another approach to investigate the characteristics of Surface Integrity parameters proceeds from a thermo-

mechanical point of view. In various literature sources, scientists proof certain measures being either thermally or mechanically induced or a result of a combination of both. The theory, that certain cutting conditions (which include the parameter of tool wear as a change in the original cutting conditions) lead to defined process forces and temperatures is a fundamental assumption for the present work. Figure 1 summarizes the relationships between the described aspects.

As suggested for the link between the thermo-mechanical load acting on the cutting edge and the Surface Integrity on the machined feature, the relationship is of statistic nature. Whereas theoretical models and simulations assume perfectly defined conditions, i.e. a precise cutting edge geometry, stable cutting conditions, flawless material models etc., real systems are always subject to variations. Despite deviations, however, the hypothesis that a thermo-mechanical load spectrum acting on the work piece material leads to particular Surface Integrity parameters occurring to a certain extent by a certain probability could be proved right.

Whilst cutting conditions are even deliberately adjusted or can easily be determined, the thermo-

mechanical load spectrum is a not directly accessible intermediate variable of the process. For the majority of industrial processes, it is neither known nor are there any efforts to directly control these parameters. Under laboratory conditions, cutting forces are measured since decades and serve for process analysis and optimization. Precise temperature measurements in contrast are far more difficult to accomplish. Calorimetric measurements, measurements using resistance thermometers or thermo-couples have been performed since the 1920s. Capturing accurate temperature values or even distributions, however, is still a challenge for engineers to date. The temperature modeling efforts, which started in the 1950s were not least driven by the high complexity of measuring temperature in a machining process.

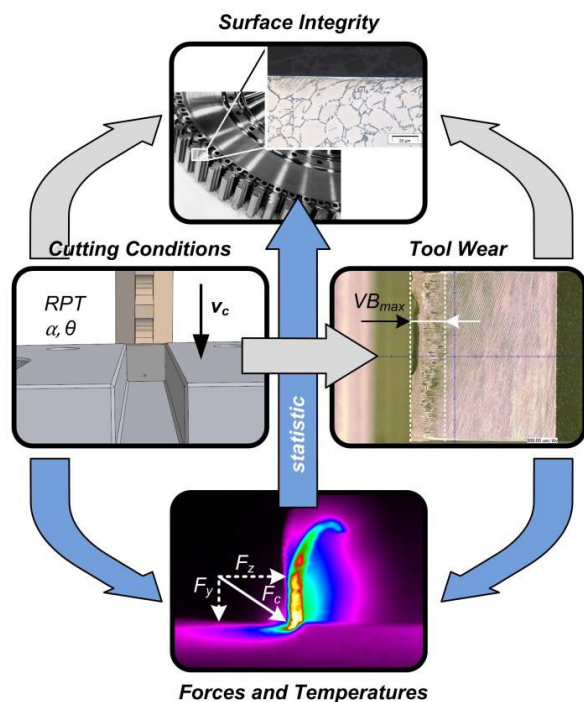


Fig. 1. Overview of the relationship between cutting conditions, tool wear and Surface Integrity

Thermography is certainly the most effective way to collect temperature information, albeit metal cutting processes, i.e. high temperature gradients, quick moving heat-sources and very low object emissivities push state-of-the-art technology to its limits. In addition, optical temperature measurement methods require a direct access to the object of interest which limits their area of application to mere laboratory conditions. In order to make the temperature information in the cutting zone available for industrial machining processes, temperature models provide an effective opportunity. In the present

article, the development of a temperature model is described which utilizes process forces indicating the total energy converted by the machining process.

## 2. State of the Art

### 2.1. Analytical temperature modeling in metal cutting

The most considerable developments in analytical temperature modeling were made more than half a century ago. In 1942, Jaeger [1] and Jaeger and Carslaw in 1959 [2] focused on temperature distributions as a consequence of a semi-infinite heat source moving parallel to material. Specifications of the general solutions regarding metal cutting processes were published by Hahn in (1951) [3], Loewen and Shaw (1954) [4], Leone (1954) [5], Weiner (1955) [6] and Chao and Trigger (1955 and 1958) [7, 8]. All models are based on Jaeger's solution and are similar in their structure. In essence, they differ from each other in assumptions regarding the moving direction and velocity of the primary heat source as well as the locations of adiabatic boundary conditions for the work piece, chip and the different tool faces. The most extensive advancements to the analytical model approach were published in 2000 and 2001 by Komanduri and Hou [9, 10, 11]. In contrast to their forerunners, who assumed two bodies generating heat in sliding contact, they formulated the primary shear zone as an oblique band heat source in the material moving at cutting speed.

At the secondary heat source, i.e. friction between chip and cutting edge (tool rake face), the existing models make different assumptions regarding the heat partition ratio between both objects on the one hand and the heat intensity along the contact length on the other hand. Komanduri and Hou assumed a non-uniform heat partition ratio and (as all preceding models) a uniform heat source intensity along the tool-chip interface. Contrary assumptions have been made by Wright et al. (1980) [12] who applied a non-uniform heat source in his model and regarded uniform heat partition ratio which was empirically determined.

### 2.2. Temperature model by Komanduri and Hou

The temperature model proposed in this publication is based on the results obtained by Komanduri and Hou, thus the specific details of their approach are discussed in the following. Figure 2 gives an overview of the different subsystems. The work piece model considers the primary heat source, i.e. shear zone only. In order to generate an adiabatic boundary at the transition of work piece to environment, a mirror heat source is introduced. For this subsystem, the valid parameter space is limited to the work piece (I), as any effect occurring in the

imaginary part is of no physical relevance. The second system focuses on the chip (II). Here, the imaginary heat source is mirrored by the transition of the chip to environment. The speed of the chip is thereby equal to the cutting speed reduced by the chip thickness ratio. The parameter  $B$  describes the heat partition ratio between the systems chip and work piece where  $B$  is the fraction going into the work piece and  $(1-B)$  the fraction going into the chip.

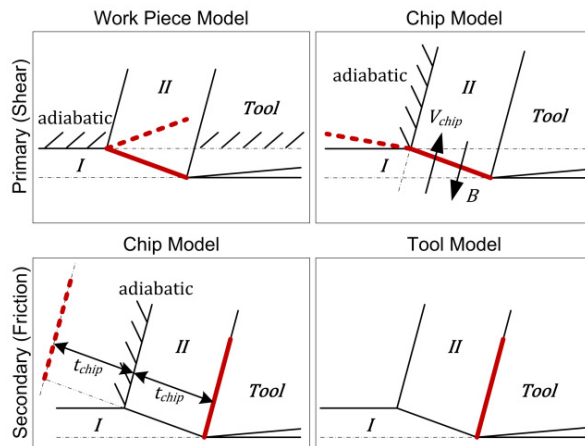


Fig. 2. Subsystems of the temperature model after Komanduri and Hou [9, 10, 11]

As the chip is at the same time influenced by the secondary heat source, the temperature field is computed for the friction at the contact length as well. In order to generate the same adiabatic boundary as in the latter case, the image heat source is parallel arranged in twice the chip thickness. The final subsystem considers the temperature distribution in the tool. In the model approach suggested by Komanduri and Hou, the only thermal input to the tool can logically take place in the contact zone to another object, i.e. the chip. Due to the fact, however, that the impact of the primary heat source cannot be simply neglected, they assumed both heat sources superimposed upon each other in the tool chip contact when calculating the temperature field in the tool. The length of the primary heat source is therefore set to the length of the secondary source and its intensity uniformly distributed along this new effective length.

In their publications, Komanduri and Hou selected individual coordinate systems for all subsystems i.e. work piece (I), chip (II) and tool in such way, that the mathematical expressions could be written as simple as possible. In order to get the overall picture, the single temperature maps were superpositioned in a joint coordinate system. A detailed description how this was realized is not mentioned. In 2013, Karas et al. [13] modified the equations so that all subsystems could be regarded in the same system of axes.

### 3. Model Specialization

#### 3.1. Reflection of Komanduri and Hou model approach regarding special case Broaching Nickel-based alloys

For the regarded case of broaching Nickel-based alloys using High-Speed-Steel tools, cutting speeds are relatively low compared to other machining processes as the thermal stability of the cutting material is at its limit at 10m/min. More important in terms of the presented temperature model is the cutting thicknesses, i.e. the rise-per-tooth ( $RPT$ ) ranging from 0.08 mm for roughing to 0.02 mm (and lower) for finishing conditions. For regrinding purposes, broaching tool sets have a calibration part in the final tool section, which exhibits a nominal  $RPT$  of zero. Even though the tools are not supposed to take a chip, the calibration teeth actually do cut material since there is a part displacement as a consequence of material relaxation. In summary the cutting thicknesses are rather low compared to most other machining processes.

The assumption of shear and frictional heat sources in the tool model combined by superposition is a simplification delivering acceptable results when the length of both heat sources is in the same order of magnitude. This may be the case for a wide range of machining processes. Due to the low cutting thicknesses in broaching, the primary heat source can be of considerably lower length compared to the tool chip contact length. This leads to a higher concentration of heat near the tool tip, which is not regarded by the existing tool model approach. For that reason, an alternative tool model has been developed, which considers the influence of both sources at their original locations for temperature field determination in the tool.

#### 3.2. Development of a tool model using independently parameterized heat sources

The model developed in the present article focuses on the temperature distribution in the cutting tool. A schematic illustration of the heat source arrangement is given in Figure 3. The origin of the coordinate system was defined at the tip of the cutting edge. Different to the Komanduri and Hou, the rake face is not rotated into the  $z$ -axis. This introduces few more parameters into the equation, however, allows to regard the entire system in its original orientation. Nevertheless, the main distinction from the existing models is the possibility to regard two independent heat sources (shear and friction) which can be separately parameterized, i.e. have different length as well as intensities. Furthermore, an adiabatic boundary was introduced for the clearance face of the cutting edge through mirroring both heat sources by the clearance plane. This was not the case for the

preceding model approaches, however, makes sense as there is no direct conductive heat transfer into the work piece possible.

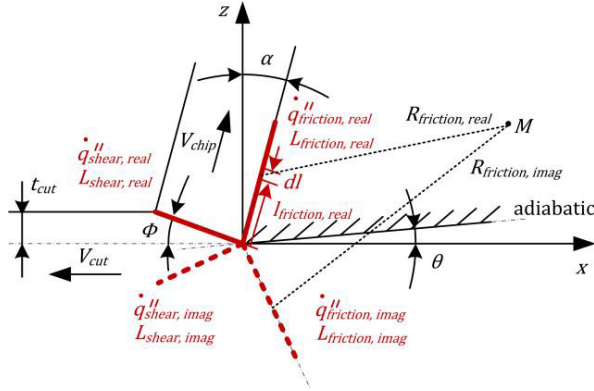


Fig. 3. Tool model using independently parameterized primary and secondary heat sources

The appropriate mathematical equation for the calculation of the temperature in the Point M for the presented semi-infinite case is given below.

$$T = \frac{\xi_{frict} \cdot \dot{q}''_{frict}}{2\pi\lambda_{tool}} \int_0^{l_{frict}} \left( \frac{1}{R_{frict,real}} + \frac{1}{R_{frict,imag}} \right) dl_{frict} + \frac{\xi_{shear} \cdot \dot{q}''_{shear}}{2\pi\lambda_{work}} \int_0^{l_{shear}} \left( \frac{1}{R_{shear,real}} + \frac{1}{R_{shear,imag}} \right) dl_{shear} \quad (1)$$

with:

$$R_{frict,real} = \sqrt{[x - l_{frict} \sin(\alpha)]^2 + [z - l_{frict} \cos(\alpha)]^2}$$

$$R_{frict,imag} = \sqrt{[x - l_{frict} \sin(\alpha + 2\theta)]^2 + [z + l_{frict} \cos(\alpha + 2\theta)]^2}$$

$$R_{shear,real} = \sqrt{[x + l_{shear} \cos(\phi)]^2 + [z - l_{shear} \sin(\phi)]^2}$$

$$R_{shear,imag} = \sqrt{[x + l_{shear} \cos(\phi + 2\theta)]^2 + [z + l_{shear} \sin(\phi + 2\theta)]^2}$$

Having completed the transformation of coordinates, Karas et al. proved their results using the same parameters as Komanduri and Hou. An overview of the parameters can be found in [13] (p. 563, top). In their publication, they plotted the temperature map for the system of work piece, chip and cutting edge and received a perfect match of both models. In order to illustrate the difference between the original model and the approach developed in the present work, the same parameters were used for comparison.

### 3.3. Comparison of the different model approaches

Figure 4 presents the temperature maps in a semi-infinite case for the tool subsystem. On the left-hand side, the modified model was used for calculation, the outcome of the original model approach is shown on the right-hand side. Both temperature maps are plotted in their own coordinate systems. For clarification, the rake plane as well as the clearance plane are drawn and the imaginary parts of the temperature fields are dismissed. Within the shape of the cutting edge, the temperature distribution is represented by isotherms.

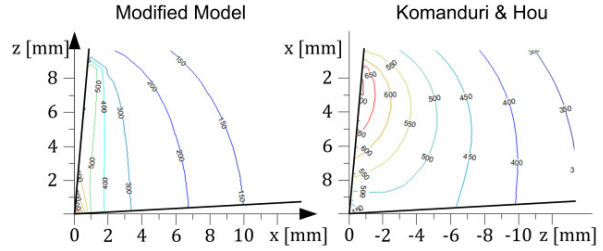


Fig. 4. Comparison of the temperature maps for the semi-infinite tool subsystem computed with the different model approaches

At first it is noticeable that the new model approach has the temperature peak value right at the tip of the cutting edge rather than on the rake face, as it is the case for the original model by Komanduri and Hou. Moreover, the overall temperatures in the modified case are considerably lower, as the heat transfer from the primary source into the cutting edge is attenuated. Because the presented temperature fields have not been validated with experimental data, it is difficult to state, which model obtains better results. Taking into account the assumptions made, however, both results make sense in its own.

## 4. Model Validation

### 4.1. Experimental set-up for measurement of the thermo-mechanical load

In order to evaluate the outcome of the different model approaches, experimental data is required. A temperature measurement on the cutting edge in one spot would allow for a conclusion about the absolute temperature level, but leave the question about the distribution open.

Thus, a FLIR SC7600 high-speed infrared camera was used in combination with a (microscope) 50mm lens providing a resolution of 15μm per pixel at 300mm working distance. Due to the fact that emissivities of the objects in view are not precisely known, a two-color pyrometer was employed measuring the absolute



temperature along the tool clearance face through a 0.5mm diameter hole in the sample work pieces 1.5mm before the exit of the cutting edge. By combination of both temperature measurement systems, it is further possible to calibrate the infrared camera images [14]. In addition, the cutting forces were recorded using a three-axial force dynamometer. An overview of the set-up is given in Figure 5 below.

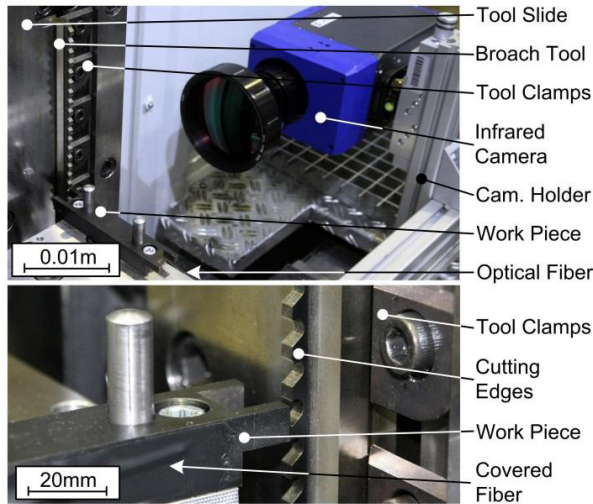


Fig. 5. Overview of the experimental set-up

The test were carried out on a Forst 8x2299x600 M/CNC electro mechanically driven broaching machine tool. The employed tools are small tool segments by industrial standards. The width of the work piece and the cutting edge were matched. The height of the Inconel 718 (triple-melt) work piece was slightly smaller than the tool pitch, so that only one cutting edge was in engagement at a time and the measurement signals can clearly be assigned to each cutting situation. To get better results for the infrared pictures, the work piece as well as the cutting edges were painted with black color.

In the experiments, different rise-per-tooth, i.e. uncut chip thickness values as well as rake angles were tested. Moreover, the cutting speed has been varied as the only free parameter in broaching, as the other parameters are integrated into the tool. Within the test series, 75 process conditions have been investigated employing 15 different broaching segments. In order to validate the model approaches in principle, one process condition is analyzed in the following section.

#### 4.2. Model validation on the basis of experimental results

The infrared camera image presented in Figure 6 was recorded when cutting at a speed of 4m/min using a tool

with a *RPT* of 0.08mm and 5° rake angle. In the upper left-hand side of the picture, the camera raw file is given showing the system of work piece, cutting edge and chip in the position 1.5mm before the exit of the tool.

Any temperature recorded by means of infrared camera systems contain (in some cases rather big) errors, because of the problems due to unknown emissivities. Especially in case of metal cutting processes where object emissivities lie in a range of 0.1 to 0.4 (whereas most cameras assume  $\varepsilon \sim 1$ ), the direct temperature output of thermography systems cannot serve for scientific questions. Thus, only the digital level differences were measured and are shown. Since a second, absolute temperature measurement system was employed, a calibration of the data is possible for all conducted measurements. Nevertheless, this elaborate step is neglected in the following, as it is not required for a qualitative validation of the model approach.

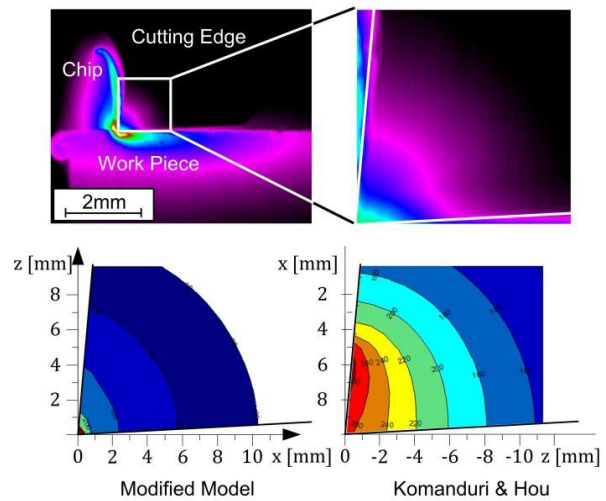


Fig. 6. Comparison of the different model approaches with experimental infrared camera image

The bottom part of the figure illustrates both temperature plots computed with the different model approaches. In both cases, the experimental values were used as parameters for calculation. Thereby, the shear angle was determined on basis of the rise-per-tooth to chip ratio, the length of the shear plane heat source geometrically calculated and the length of the frictional heat source defined using the camera images. It was further assumed that the entire energy is converted into heat. The heat sources were determined based on the measured cutting forces, cutting speed and the shear plane as follows.

$$\dot{q}'' = \frac{F \cdot v_c}{L \cdot w} \quad \text{with} \quad \dot{q}'' = \dot{q}''_{\text{shear}} + \dot{q}''_{\text{friction}} \quad (2)$$

In the new developed model, the partition of the total energy to the different heat sources was iteratively optimized to fit the experimental data in a best possible way.

Comparing both temperature maps, it is obvious that the Komanduri and Hou model approach does not reflect the process conditions in broaching Nickel-based alloys very well. The fact that the heat of both sources is introduced into the cutting edge through the rake face cannot be confirmed by means of the conducted experiments.

The modified model approach obviously considers the process conditions better. The qualitative temperature distribution is almost perfectly congruent with the one in the real image. Yet can be observed, that the isotherms cling slightly stronger to the clearance plane in the real case. It is possible that this is due to friction between work piece and the clearance face (even though the broaching tools were used in a sharp state only) which is not considered in the temperature model.

In order to better fit the experimental observations and to regard higher tool wear conditions, the introduction of a third heat source could be a further improvement of the suggested model approach.

## 5. Summary and Conclusion

In the present article, the relevance of temperature for the quality in general and Surface Integrity in particular was discussed. Furthermore, analytic approaches for temperature modeling were presented. Most notably the model approach suggested by Komanduri and Hou was identified as an outstanding tool in order to determine cutting temperatures. For the industrial application of broaching Nickel-based alloys, their model was reconsidered and modified for the calculation of the temperature over the cutting edge for the semi-infinite case. Furthermore, experimental works for temperature measurements under industrial process conditions were presented. The comparison of the model result to the experimental findings show a very good correlation.

The presented solution of the analytic model approach in combination with real-time force measurements can in a next step be merged to a process monitoring tool enabling industry to monitor temperature. As temperature has a strong impact on Surface Integrity parameters as stated above, the monitoring approach provides an effective possibility to control the part quality during machining already.

## 6. Summary and Conclusion

The work was developed within the scope of the Collaborative Research Center SFB/TR 96: “Thermo-Energetic Design of Machine Tools” and the FAA sponsored program “Process Monitoring Strategies in Turning and Broaching for Implementation of New Designs and Materials in Turbine Engines”.

## References

- [1] Jaeger, J.C., 1942. Moving Sources of Heat and the Temperatures at Sliding Contacts, *Proceedings of Royal Society of NSW*, 76, pp. 203-224.
- [2] Carslaw, H.S., Jaeger, J.C., 1959. *Conduction of Heat in Solids*, Oxford, UK, Oxford University Press.
- [3] Hahn, R.S., 1951, On the Temperature Development at the Shear Plane in the Metal Cutting Process, *Proceedings of First National Congress of Applied Mechanics*, pp. 661-666
- [4] Loewen E.G., Shaw, M.C., 1954, On the Analysis of Cutting Tool Temperatures, *ASME Transactions of American Society of Mechanical Engineers*, 76, pp. 217-231.
- [5] Leone, W.C., 1954, Distribution of Shear Zone Heat in Metal Cutting, *ASME Transactions of American Society of Mechanical Engineers*, 76, p. 121-125.
- [6] Weiner, J.H., 1955, Shear Plane Temperature in Orthogonal Machining, *ASME Transactions of American Society of Mechanical Engineers*, 77, pp. 1331-1341.
- [7] Chao, B.T., Trigger, K.J., 1955, Temperature Distribution at the Tool-Chip Interface in Metal Cutting, *ASME Transactions of American Society of Mechanical Engineers*, 77, 2, pp. 1107-1121.
- [8] Chao, B.T., Trigger, K.J., 1958, Temperature Distribution at Tool-Chip and Tool-Work Interface in Metal Cutting, *ASME Transactions of American Society of Mechanical Engineers*, 20, 1, pp. 311-320.
- [9] Komanduri, R., Hou, Z.B., 2000, Thermal Modeling of the Metal Cutting Process, Part I: Temperature Rise Distribution due to Shear Plane Heat Source, *International Journal of Mechanical Sciences*, 42, pp. 1715-1752.
- [10] Komanduri, R., Hou, Z.B., 2001a, Thermal Modeling of the Metal Cutting Process, Part II: Temperature Rise Distribution due to Frictional Heat Source at the Tool-Chip Interface, *International Journal of Mechanical Sciences*, 43, pp. 57-58.
- [11] Komanduri, R., Hou, Z.B., 2001b, Thermal Modeling of the Metal Cutting Process, Part III: Temperature Rise Distribution due to the Combined Effects of Shear Plane Heat Source and the Tool-Chip Interface Frictional Heat Source, *International Journal of Mechanical Sciences*, 43, pp. 89-107.
- [12] Wright, P.K., McCormic, S.P., Miller, T.R., 1980, Effect of Rake Face Design on Cutting Tool Temperature Distributions, *ASME Journal of Engineering for Industry*, 102, 2, pp. 123-128.
- [13] Karas, A., Bouzit, M., Belarbi, M., 2013, Development of a Thermal Model in the Metal Cutting Process for Prediction of Temperature Distributions at the Tool-Chip-Workpiece Interface, *Journal of Theoretical and Applied Mechanics*, 51, 3, pp. 553-567.
- [14] Gierlings, S., Brockmann, M., 2013, Analytical Modeling of Temperature Distribution using Potential Theory by Reference to Broaching Nickel-Based Alloys, *Advanced Material Research*, Vol. 769, ISSN 1662-8985, pp. 139-146.